

Thermal Activation and Saturation of Ion Beam Sculpting

David P. Hoogerheide¹, H. Bola George², Jene A. Golovchenko^{1,2} & Michael J. Aziz^{2*}

¹*Physics Department, Harvard University, Cambridge, MA 02138*

²*Harvard School of Engineering & Applied Sciences, Cambridge, MA 02138*

We report a material-dependent critical temperature for ion beam sculpting of nanopores in amorphous materials under keV ion irradiation. At temperatures below the critical temperature, irradiated pores open at a rate that soon saturates with decreasing temperature. At temperatures above the critical temperature, the pore closing rate rises rapidly and eventually saturates with increasing temperature. The observed behavior is well described by a model based on adatom diffusion, but is difficult to reconcile with an ion-stimulated viscous flow model.

* Corresponding author. Email: maziz@harvard.edu; Telephone 617-495-9884; Fax 617-495-9837

Introduction

Ion beams are effective tools for controlling surface morphologies down to molecular dimensions. Combined with complementary techniques such as surface self-assembly, they are envisaged to play a significant role in large-scale production of nanodevices. This promise has already been realized in the use of low-energy ion beams to controllably reduce the diameter of silicon nitride nanopores from large fractions of microns to the single-digit nanometer scale.¹ Such *ion-sculpted* nanopores are useful for detecting properties of single biomolecules and are a potential framework for rapid DNA sequencing of single molecules.²

The mechanism of ion sculpting remains unclear, as the sculpting of nanopores in non-stoichiometric (low-stress) SiN_x , amorphous and crystalline Si (*a*-Si and *c*-Si), SiO_2 , and palladium silicide led to an array of observations which in total are difficult to reconcile within the context of a single mechanism. One hypothesized mechanism is the creation by the ion beam of mobile species (called “adatoms”) on the surface, which independently diffuse along the surface until annihilated. One of the annihilation channels is an adatom sink at the edge of the pore, thereby acting to close it through adatom accretion. The adatom diffusion model developed to explain this effect accounts well for the observed high sensitivity to temperature T . It also accounts well for the increased efficiency of closing of nitride and oxide pores at low beam fluxes or with flux pulsing;^{1,3} and explains qualitatively why “nano-volcanoes”—enormous accretions of material at nitride pore edges—appear to interact with each other over microns of distance.⁴

Other observations are difficult to explain with the adatom diffusion mechanism. Only amorphous materials, or materials that become amorphous under irradiation, exhibit nanopore closure.⁵ Moreover, the closing rate of a nanopore displays a “memory effect” wherein it

depends not only on the pore's instantaneous size, but also on its initial size.⁶ These observations are better explained by another hypothesized mechanism^{1,6}: the creation by the ion beam of a very thin, stressed viscous surface layer, where compressive stress caused by the ion beam is relieved; viscous flow of the thin surface layer with a viscosity reduced by ion irradiation acts to close the pore. The viscous flow model explains the restriction to amorphous materials and accounts quantitatively for the memory effect.⁶

In this Article, we report a study of nanopore opening and closure in SiN_x, amorphous Si (*a*-Si), and crystalline Si (*c*-Si). We observe a critical temperature T_c above which pores close, and three temperature regimes. At low T , pores open at a temperature-independent rate. At temperatures near and above T_c , pore closing rates increase rapidly with increasing temperature. At high T , pore closing rates saturate. These observations are shown to be quantitatively consistent with the adatom diffusion model but are difficult to reconcile with the viscous flow model.

Experimental methods

For the ion sculpting experiments on nitride surfaces, samples were 200-nm thick low-pressure chemical vapor deposition (LPCVD) grown non-stoichiometric SiN_x on Si(001) substrates. Membranes 50 $\mu\text{m} \times 50 \mu\text{m}$ were fabricated by a series of photolithography and wet etching steps. Oxide membranes were 500 nm thick thermal oxide on Si(001). Crystalline Si free-standing membranes were fabricated from silicon-on-insulator (SOI) substrates. The initial pores were milled in the free standing membranes using a 50 keV Ga²⁺ focused ion beam (FIB) machine. Amorphous Si nanopores were formed by sputter depositing *a*-Si onto a 700-nm pore in a free-standing oxide membrane. Fabrication details for all samples are provided elsewhere.⁵

The ion sculpting apparatus has been described in detail elsewhere;^{1,7} the Kaufmann-source Ar^+ ion beam is operated at 3 keV in continuous mode at normal incidence. With differentially-pumped argon flowing into the ion gun chamber at 1.5×10^{-6} Torr, the sample chamber base pressure is less than 10^{-7} Torr. The pore area is determined in real time from the initial pore area (determined by transmission electron microscopy) and the instantaneous counting of the Ar^+ ions going through the pore. The sample temperature is controlled to within 1 °C using a local resistive heater and liquid nitrogen refrigeration.

Results and Discussion

To investigate the role of temperature on the pore closing dynamics, we cycled the temperature at constant flux between -80 and 95 °C. We alternated between high (pore closing) and low (pore opening) temperatures to evaluate the temperature-dependence of the closing rate at a roughly constant pore size. In Fig. 1 we show typical pore area vs. fluence results as the temperature is cycled, in this case for the *c*-Si nanopore.

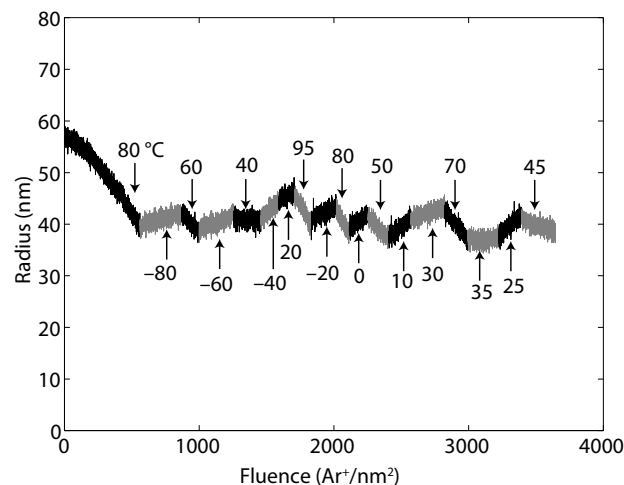


Fig. 1: Evolution of *c*-Si nanopore radius during temperature cycling. Shading is alternated to demarcate constant temperature regions.

Earlier experiments by Li *et al.*¹ showed that silicon nitride nanopores exhibit a critical temperature T_c below which the pores opened at a constant rate and above which the closing rates were temperature-dependent. Our present results, extending the temperature range compared to the earlier work by Li *et al.*, show the onset of a high saturation temperature, $T_{sat} > T_c$, above which the pores close at a high, temperature-independent rate. As shown in Fig. 2, this temperature effect is not limited to silicon nitride, but appears to be a universal feature: similar trends are observed with both amorphous and crystalline Si pores.

Although the temperature-dependence expected from the viscous flow model is currently unpredictable, the measured temperature dependence can be compared quantitatively with that predicted by the adatom diffusion model, in which the rate of closure of a pore of radius R with fluence ϕ is described by¹

$$\frac{dR}{d\phi} = -\frac{\Omega R}{H} \left(Y_a \left(\frac{X_m}{R} \right) \frac{K_1 \left(\frac{R}{X_m} \right)}{K_0 \left(\frac{R}{X_m} \right)} - Y_p \right), \quad (1)$$

where X_m is a characteristic distance the adatoms diffuse before annihilation by the beam or immobilization in surface traps; K_i is the i^{th} order modified Bessel function of the second kind, and H , Ω , Y_a and Y_p are the film thickness, atomic volume, adatom yield and sputter yield, respectively. The first term on the r.h.s. accounts for closure as the adatoms diffuse to the pore edge and the second describes the opening rate due to sputter erosion.

Each of the parameters in equation 1 can be calculated or estimated from the experimental parameters. Following Li *et al.*, we take the film thickness H to be approximately the pore length, which is estimated to be 10 nm from ionic conductance measurements.¹ The volume Ω of

silicon is 0.02 nm^3 per Si atom. Finally, we make an order-of-magnitude estimate of the adatom production rate to be about 10 adatoms per incident ion.⁸ We will discuss X_m and Y_p below.

In the adatom diffusion model, X_m depends on the surface diffusivity D according to

$$\frac{1}{X_m^2} = \frac{1}{\ell_{trap}^2} + \frac{\sigma}{D} f, \quad (2)$$

where f is the ion flux, σ is the cross section for adatom annihilation by an impinging ion, and ℓ_{trap} is the average distance between surface defects that might trap an adatom.

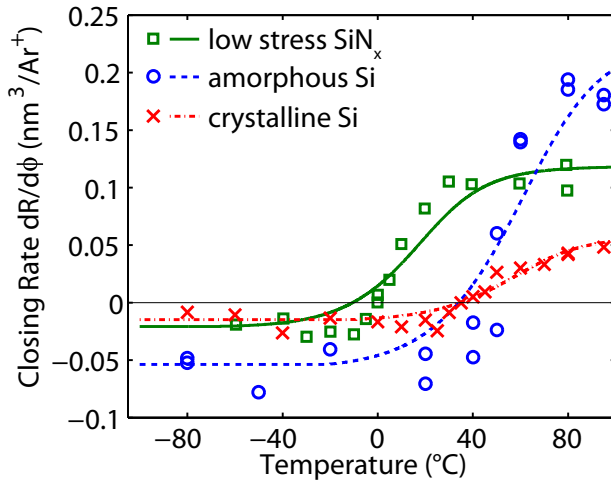


Fig. 2: (Color online) Temperature dependence of pore closing rates of ion-sculpted SiN_x , a -Si, and c -Si pores with ion flux $f = 0.24 \text{ Ar}^+ \text{ nm}^{-2} \text{ s}^{-1}$. Smooth curves are least-squares fits to the adatom diffusion model.

Temperature dependence enters the model through the diffusivity D . We assume an Arrhenius form to the diffusivity, $D = D_0 \exp(-E_d/kT)$. At sufficiently high temperature, the diffusivity is high, the second term on the r.h.s. of (2) is negligible, X_m saturates at ℓ_{trap} , and the closing rate becomes temperature-independent. At sufficiently low temperature, the diffusivity is suppressed, the first term on the r.h.s. of (2) is negligible, and X_m approaches zero. At low

temperatures, then, the first term in brackets of Eq. (1) is also zero, and we estimate Y_p from the average of low-temperature measurements of the opening rates:

$$Y_p = -\frac{H}{\Omega} \left\langle \frac{1}{R} \frac{dR}{d\phi} \right\rangle, \quad (3)$$

where the angle brackets denote the average over temperatures below -5 °C, 30 °C, and 20 °C for SiN_x , $a\text{-Si}$, and $c\text{-Si}$, respectively. Values of Y_p are tabulated in Table 1. These are somewhat smaller than the sputtering yields of about 2.3 atoms/ion for SiN_x and 1.1 atoms/ion for silicon predicted by a SRIM⁹ calculation but are not unreasonable.

The lines in Fig. 2 represent a fit of the adatom diffusion model to the data with two adjustable parameters: ℓ_{trap} and E_a . We assumed a typical value for the surface diffusivity prefactor, $D_0 = 10^{-3}$ cm²/s. Parameters not treated as adjustable were the annihilation “footprint”¹ of $\sigma = 0.1$ nm², Y_p , and the experimental beam flux $f = 0.24$ Ar⁺/nm²/s. Best-fit values for the activation energies and average trap distances are given in Table 1.

Table 1. Experimental and fit parameters for adatom diffusion model.

Material	SiN _x	a-Si	c-Si
Initial pore radius (nm)	74	165	59
Average pore radius (nm)	30	102	41
Y_p (atoms/Ar ⁺)	0.73	0.28	0.20
T_c (°C)	0	45	35
E_a (eV)	0.62	0.72	0.78
ℓ_{trap} (nm)	12.0	13.4	3.5

The adatom diffusion model also predicts that T_c increases with pore radius and ion flux. The bracketed term in Eq. (1) is zero at T_c , so if Y_p is temperature-independent then so must be X_m/R .

The characteristic diffusion distance before annihilation, X_m , increases with T and decreases with flux (due to the enhanced annihilation rate). Because X_m must increase with R to maintain a constant ratio at T_c , T_c must increase with R . Also, because increasing the flux decreases X_m , a corresponding temperature boost is required to bring X_m/R back to the necessary value to keep the bracketed term zero. We have observed these qualitative trends for 3 keV Ne^+ irradiated silicon nitride pores.

Although the adatom diffusion model fits the data with physically reasonable parameter values¹⁰ and provides an intuitive explanation of the three temperature regimes, significant difficulties remain. The width of the measured transition from opening to saturated closing in Fig. 2 is sharper than predicted for reasonable diffusion pre-exponential factors accompanied by small activation energies: treating both D_0 and E_a as adjustable parameters results in better fits, but with much larger values of E_a and unphysically large values of D_0 .

Furthermore, studies of c -Si following ~ 1 keV Ar^+ irradiation near room temperature have established that a surface layer of thickness roughly (range + standard deviation) rapidly becomes amorphous.¹¹ The temperature at which the surface remains fully crystalline under irradiation is estimated⁵ to exceed 500 °C. Hence it is difficult to reconcile any surface diffusion model with the factor of ~ 3 difference between observed rates in a -Si and c -Si. The viscous flow model is almost as difficult to reconcile to these results: if the flowing region is limited to an amorphous layer of thickness (range + standard deviation), then behavior should be identical for nanopores that are initially c -Si or a -Si. If, however, in the a -Si film, there is some fluidity in deeper regions, perhaps due to point defects injected from ion irradiation, then flow could be more facile in the fully amorphous films and pores could close faster than in the ion beam surface-amorphized c -Si films.

The strong temperature-enhancement of the closing rate, which is readily explained by the adatom diffusion model, cannot arise from a viscous flow model through a temperature-enhanced fluidity: Hutchinson and coworkers have shown that the evolving shape of the pore is affected negligibly by the elasticity and the viscosity in the viscous flow model⁶. A temperature dependence could enter this model through the temperature-dependence of the magnitude of anisotropic deformation induced per unit of fluence. This has been observed to decrease smoothly with increasing temperature¹² in SiO₂, but a temperature-dependence of the opposite sign and with an unprecedented structure would be required to account for the three temperature regimes that we report here. It is possible that a superposition of the two mechanisms may be necessary to account for all the observations.

A potentially important influence on the closing dynamics is the formation of nanoscale volcanoes, which has been observed in SiN_x¹³, SiO₂¹⁴ and a-Si¹⁴. The volcano size in SiN_x nanopores has been observed to depend strongly on the sample closing temperature, and may increase with temperature more rapidly as the closing rate is saturating. Volcano growth may compete for mass with pore closure, and volcanoes may be a possible mechanism for the “memory effect”: a pore’s closing rate may depend on both its instantaneous size and its initial size because the volcano size may depend on both.

Conclusion

Ion-irradiated nanopores in *a*-SiN_x, *a*-Si, and *c*-Si films close above a critical temperature and open below it, exhibiting three temperature regimes: a low-*T* regime in which the opening rate is temperature-independent; an intermediate-*T* regime spanning from slightly below to well above the critical temperature, wherein the closing rate increases rapidly with increasing

temperature; and a high- T regime in which the closing rate is temperature-independent. The adatom diffusion model fits the measured rates with physically reasonable parameter values, whereas the ion-induced viscous flow model does not exhibit multiple temperature regimes. Neither an adatom diffusion picture nor an ion-induced viscous flow picture is consistent with all of the observations. Further research will be required to settle these issues.

Acknowledgments: D.P.H. and H.B.G. contributed equally to this work. We acknowledge assistance from Marc Gershow, Slaven Garaj, Joost Vlassak and Xi Wang. D.P.H acknowledges support from the NSF, and NDSEG, and, together with J.A.G., the NIH National Human Genome Research Institute awards #5R01HG003703 and #3R01HG003703-05S1 to J.A.G. The work of H.B.G. and M.J.A. was supported by the U.S. Department of Energy through grant DE-FG02-06ER46335. This work was performed in part at the Center for Nanoscale Systems at Harvard University member of the National Nanotechnology Infrastructure Network, which is supported by the NSF under award no. ECS-0335765.

References

- ¹J. Li, D. Stein, C. McMullan, D. Branton, M.J. Aziz, and J. Golovchenko, *Nature* **412**, 166 (2001).
- ²J. Li, M. Gershow, D. Stein, E. Brandin, and J.A. Golovchenko, *Nature Materials* **2**, 611 (2003).
- ³D. Stein, J. Li, and J.A. Golovchenko, *Phys. Rev. Lett.* **89**, 276106 (2002).
- ⁴T. Mitsui, D. Stein, Y.R. Kim, D. Hoogerheide, and J.A. Golovchenko, *Physical Review Letters* **96**, 036102 (2006).

⁵H.B. George, D.P. Hoogerheide, C.S. Madi, D.C. Bell, J.A. Golovchenko, and M.J. Aziz, Appl. Phys. Lett. **96**, 263111 (2010).

⁶H.B. George, Y. Tang, X. Chen, J. Li, J.W. Hutchinson, J.A. Golovchenko, and M.J. Aziz, J. Appl. Phys. **108**, 014310 (2010).

⁷D. Stein, C. McMullan, J. Li, and J. Golovchenko, Rev. Sci. Instrum. **75**, 900 (2004).

⁸J.M. Pomeroy, J. Jacobsen, C.C. Hill, B.H. Cooper, and J.P. Sethna, Phys. Rev. B **66**, 8 (2002).

⁹J.F. Ziegler, J.P. Biersack, and U. Littmark, *The Stopping and Range of Ions in Solids*. (Pergamon, New York, 1985).

¹⁰Y.W. Mo, J. Kleiner, M.B. Webb, and M.G. Lagally, Phys. Rev. Lett. **66**, 1998 (1991).

¹¹C.S. Madi, unpublished

¹²M.L. Brongersma, E. Snoeks, T. van Dillen, and A. Polman, Journal of Applied Physics **88**, 59 (2000).

¹³D.P. Hoogerheide and J.A. Golovchenko, Mater. Res. Soc. Symp. Proc. **1020**, paper #1020 (2007).

¹⁴H.B. George, Ph.D. Thesis, Harvard University, 2007.